



Seismic assessment of nineteenth and twentieth centuries URM buildings in Lisbon: structural features and derivation of fragility curves

A. G. Simões¹ · R. Bento¹  · S. Lagomarsino² · S. Cattari² · P. B. Lourenço³

Received: 10 November 2018 / Accepted: 10 April 2019 / Published online: 15 April 2019
© Springer Nature B.V. 2019

Abstract

The article addresses the seismic vulnerability assessment of a typology of unreinforced masonry buildings constructed in Lisbon between the nineteenth and the twentieth centuries. The main architectural and structural features of these buildings are presented. This supported the identification of the main uncertainties affecting their seismic performance and the definition of classes of buildings representative of the typology. The seismic assessment includes the generation of fragility curves that combine the in-plane and out-of-plane response following different criteria and methods of analyses. The results put in evidence the seismic vulnerability of this class of buildings. Considering the earthquake-resistant code for Lisbon with a return period of 475 years, about 50% probability of having heavy damage and about 30% probability of collapse were estimated. The structural intervention on these buildings is urgent in order to reduce losses due to future earthquakes. Further studies for the assessment of similar buildings in Lisbon and elsewhere can be developed using the adopted procedure.

Keywords Unreinforced masonry buildings · Uncertainty analyses · Performance-based seismic assessment · Non-linear analyses · Fragility curves

✉ R. Bento
rita.bento@tecnico.ulisboa.pt

A. G. Simões
ana.g.simoies@tecnico.ulisboa.pt

S. Lagomarsino
sergio.lagomarsino@unige.it

S. Cattari
serena.cattari@unige.it

P. B. Lourenço
pbl@civil.uminho.pt

¹ CERIS, Instituto Superior Técnico, Universidade de Lisboa, Av. Rovisco Pais, 1049-001 Lisbon, Portugal

² DICCA, Università degli Studi di Genova, Via Montallegro 1, 16145 Genoa, Italy

³ ISE, Universidade do Minho, Campus de Azurém, 4800-058 Guimarães, Portugal

1 Introduction

In the last decades, the simplification of the normative for the rehabilitation of buildings (e.g. Decree-Law No 32, from 2012, which clearly refer that the urban rehabilitation of existing buildings does not need to respect the legislation after the original construction), the fiscal benefits and the increase of funding allowed for more investment in the urban regeneration of Lisbon and many other historic cities in the world. The decrease of construction of new buildings in the outskirts of Lisbon and the real estate speculation in the city centre have contributed to modify the focus of the construction industry. These changes require knowledge about the existing stock of buildings and call for state-of-the-art rehabilitation processes to guarantee safety, functionality and the maintenance of cultural features. According to the building census in 2011 (INE 2012), Lisbon has about 53,000 buildings. From these, 57% feature load-bearing masonry walls.

The residential unreinforced masonry (URM) buildings constructed in Lisbon between the nineteenth and the twentieth centuries (usually called *Gaioleiro* buildings) characterize a period of low construction quality and medium rise buildings (between four and six storeys). This is evident when in comparison with the preceding earthquake-resistant masonry buildings constructed after the 1755 earthquake (Lopes et al. 2014). This article addresses the seismic assessment of these URM buildings and deals with the evaluation of the uncertainties that mostly influence the structural performance of the buildings.

To this aim, the main architectural and structural features of these URM buildings are firstly presented. This includes information about the configuration of the buildings, structural systems, constructive details and characterization of materials based on the application of the Bayes Theorem. This characterization is the starting point to define representative classes of buildings. Then, the dynamic characteristics of the models used to perform the non-linear analysis are compared with the experimental dynamic characteristics obtained from ambient vibration tests.

Fragility curves are subsequently derived based on non-linear analysis and detailed models, combining the global and the local response of the structure, considering epistemic and aleatory uncertainties. The first type of uncertainties aims to account for the incomplete knowledge about the structure of the buildings and is herein treated by the logic-tree approach. The second type of uncertainties deals with the quantification of specific parameters and the intrinsic variations between buildings. The aleatory variables associated with the global and local response are, respectively, treated by the Monte Carlo Method (Rubinstein 2011) and by the Response Surface Technique (Liel et al. 2009). The generated fragility curves are then compared with curves present in the literature.

2 Architectural characterization

2.1 Historical background

The Lisbon urban development plans in 1889 originated new aggregates of buildings in the northern area, known as “*Avenidas Novas*” (meaning New Avenues). During the nineteenth century, multi-storey residential buildings were commonly constructed for renting. On the transition to the twentieth century, the idea of rentable buildings changed. The liberal bourgeoisie preferred to buy the already finished buildings and use them as a “financial

product”. Filius Populi (anonymous author under a pseudonym), claims that contractors from Tomar, a small city 150 km from Lisbon, were responsible for a new system of buildings “for sale”, where the profit of the transaction would be maximized using cheaper materials and construction processes. Additionally, Portugal suffered bankruptcy in 1892 and moved from a monarchy to a republic in 1910. The devaluation of the currency, the subsequent inflation in material prices and the shortage of credit, forced contractors to purchase cheaper materials and to simplify the construction processes. Some of these buildings even collapsed during the construction phase (Simões et al. 2017). This caused, in 1921, a public demonstration against the so-called “gaoieiros”, the name given to the contractors which were seeking for fast profit and were constructing buildings without guaranteeing the minimum safety conditions. After a few years, the URM buildings of this period got to be known as “gaoieiro” buildings in a pejorative way, meaning “bird cage”, as they seemed more adequate for birds than people (Appleton 2005; Simões et al. 2017).

2.2 Urban design and configuration of the buildings

The city expansion plan of 1889 was more flexible than the preceding “Pombalino” reconstruction plan, which followed the 1755 earthquake in Lisbon (Lopes et al. 2014). In the second half of the nineteenth century, no specifications were provided regarding the aesthetics of the new urban areas, the configuration of the buildings or the health conditions of the houses.

The buildings from this period are located along the perimeter of the blocks, with entrances facing the street and private courtyards in the rear of the building (Simões et al., 2017). They were constructed side by side or with small passageways in between, to access the courtyards. The street façades are characterized by a diversity of proportions and architectural or decorative solutions following the requests of an emerging bourgeoisie. The lower level has large entrance doors and was used for stores (Fig. 1a). Bush-hammered limestone was usually adopted as finishing. The medium level corresponds to flats. It is often plastered and painted or finished with ceramic tiles (Fig. 1b). The top level includes the cornice and parapet (sometimes a balustrade) and the roof with dormer windows or mansards. The buildings are decorated with terracotta/moulded reliefs or glazed tiles with

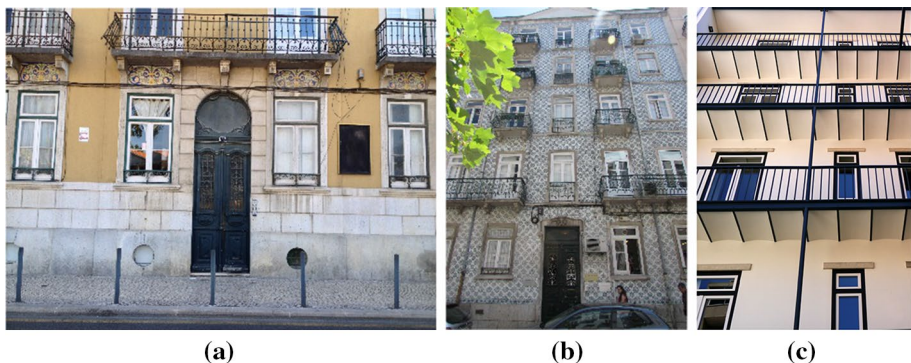


Fig. 1 Image of the buildings (Simões et al. 2017): street façade with **a** limestone stone and **b** ceramic tiles, and rear façade with **c** steel balconies

floral motifs, in friezes or around the windows and exuberant steelwork, in cast or wrought iron, is used in doors, fences, balustrades and gates.

The rear façades are much simpler and mainly intended to service functions (such as laundry). The finishing of the walls is made of plaster and painting. Steel and cast iron balconies with stairs are placed on the façade to access the courtyards (Fig. 1c). These are some examples of the cast-iron in residential architecture in Lisbon.

These URM buildings are, typically, five storeys and have elongated plan shapes. They can be divided into four types: type I—small size façades and one flat per floor; type II—medium size façades and one flat per floor; type III—medium to large façades and two flats per floor; and type IV—corner of the block with one or two flats per floor. This classification has been proposed in (Appleton 2005). Buildings type I to III are characterized by long corridors connecting the rooms adjacent to the street and the rear façades. The flats have several lateral rooms with insufficient natural light and ventilation, as these depend on the depth of the lot and the size of the airshafts. Buildings of type IV are a particular case because of the position on the corner of the blocks and the use of two street façades.

3 Structural characterization

3.1 Main features

The foundation system is characterized by rubble stone masonry with larger thickness than the load-bearing walls (direct foundation). The width of the foundation varies between 0.7 and 1.5 m on the façade walls and between 0.3 and 0.8 m on the side walls and airshafts. Usually, hard limestone and air lime mortar was used.

The façade walls are made of rubble stone and air lime mortar and are typically 0.6 to 0.9 m thick at the ground floor level, decreasing between 0.05 and 0.10 m in each floor. Openings are covered by shallow relieving brick masonry arches (Fig. 2a). The side walls are made of clay brick and air lime mortar. The thickness of these walls varies between 0.20 and 0.50 m and is constant between floors.

The internal load-bearing walls are placed parallel to the façades to support the floor timber beams. These are also made of clay brick masonry and, in some cases, they are reinforced by timber elements (Fig. 2b). The partition walls are made of clay brick masonry or vertical timber boards, and horizontal laths filled with mortar (Fig. 2c).

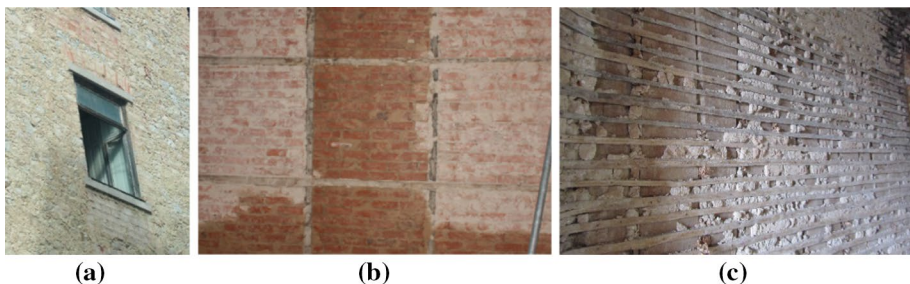


Fig. 2 Walls: **a** rubble stone masonry walls and window with clay brick relieving arch, **b** clay brick wall with timber frame and **c** timber walls

Floors are made of timber joist set perpendicular to the façades with a distance of 0.35–0.45 m between each other. The joists range between 0.07 and 0.08 m for the width and 0.16 and 0.22 m for the height. Timber joists are directly embedded on the walls or supported on transition joists with squared sections (0.07–0.10 m) running inside the wall. Floors are covered by timber boards or by hydraulic tile paving on kitchens and bathrooms. The buildings have pitched roofs with ceramic tiles supported on a simple timber structure.

In general, the weakest points of URM buildings are the poor connections (between walls or between walls and floors/roof) and the limited stiffness of timber floors (see (Simões et al. 2017)). In particular, in case of an earthquake, weak connections may cause the overturning of the façades or the collapse of the floors and/or roof. The limited stiffness of timber floors reduces the load transfer capacity between walls, leading to a lack of global behaviour.

In the last decades, several buildings have experienced alterations to their original design. For instance, there are many buildings with internal walls replaced by steel or reinforced concrete beams to create larger spaces (Fig. 3a) and buildings with the removal of masonry piers on the ground floor façade wall to open shop windows (Fig. 3b). This type of intervention introduces local weaknesses and stiffness variations on the building.

3.2 Masonry mechanical properties

The structural behaviour of URM buildings is directly dependent on the materials and constructive details and indirectly dependent on the usage and state of conservation. One of the main challenges when assessing existing buildings is the definition of the mechanical properties of the materials. There are limitations to the type and number of tests that can be conducted in situ and the restrictions to the extraction of samples for laboratory testing. Alternatively, laboratory tests on specimens constructed to represent traditional masonry walls can be carried out.

Nevertheless, the number of experimental campaigns on characterization of the materials in Lisbon URM buildings is quite limited. In Simões et al. (2017) a summary of the main experimental results is presented, considering both in situ and laboratory testing. The sample puts in evidence the dispersion of results and the difficulty to define reference values with reasonable degree of confidence. Due to this, and taking advantage of the experimental data



Fig. 3 Alterations: **a** removal of internal walls to have larger rooms and **b** removal of masonry piers to have large shop window

acquired, a plausible interval of values was defined, based on the application of the Bayesian update approach (Bracchi et al. 2016; Franchin and Pagnoni 2018).

The Bayes' Theorem is used to update the probability of a *a priori* distribution given that new evidences are available. In this case, the *a priori* distribution is defined by the interval of values proposed in the commentary to the Italian Code—NTC08 (MIT 2009) for the relevant masonry types, whereas the new evidences are defined by the experimental test results carried out in Lisbon.

Table 1 presents the reference and updated values for the modulus of elasticity (E), compressive strength (f_m) and equivalent shear strength as (τ_0) for different masonry types. The specific weight (γ) is also included. The stiffness properties presented are representative of the uncracked state. An advantage of this approach is that, when new test results become available, the interval may be easily updated. The shear modulus (G) is assumed equal to 1/3 of the modulus of elasticity, following the recommendation from (MIT 2009).

4 Seismic assessment

4.1 Description of the approach

It is proposed to analyse the seismic behaviour of buildings of type I—small size façade walls and one flat per floor—as the most representative (Simões et al. 2017). In a row of buildings, buildings of type I are located in the middle or in the end of the row. Therefore, a group of three buildings of type I is considered as case study and the behaviour of the buildings with one or two adjacent buildings and their interaction is discussed. The geometry and layout of the buildings is defined based on the average characteristics of six reference buildings from an existing block of buildings (Simões et al. 2017). This average model is replicated to define the group of three buildings (Fig. 4a, b).

For the seismic assessment, fragility curves are defined, addressing the global response of the structure, mainly governed by the in-plane capacity of the walls, and the local response, related to the activation of out-of-plane collapse mechanisms of parts of the buildings insufficiently connected to the rest of the structure. Fragility curves provide the probability of reaching or exceeding a certain limit state (LS) as a function of a selected seismic intensity measure (IM) and are herein described by a lognormal cumulative distribution function, as:

$$p_{LS}(im) = P(d \geq D_{LS} | im) = P(im_{LS} < im) = \Phi \left(\frac{1}{\beta_{LS}} \log \left(\frac{im}{IM_{LS}} \right) \right) \quad (1)$$

Table 1 Reference values for the mechanical parameters of masonry (Simões et al. 2017)

Material	Values	f_m (MPa)	E (GPa)	τ_0 (MPa)	γ (kN/m ³)
Rubble stone masonry	Ref.	1.00–1.80	0.69–1.05	0.030–0.048	19
	Updated	0.84–1.07	0.62–0.88	0.018–0.026	
Solid brick masonry	Ref.	2.40–4.00	1.20–1.80	0.060–0.092	18
	Updated	0.95–1.21	0.72–0.99	0.060–0.092	
Hollow brick masonry	Ref.	2.40–4.00	1.20–1.80	0.060–0.092	15
	Updated	0.87–1.18	0.72–0.99	0.60–0.092	

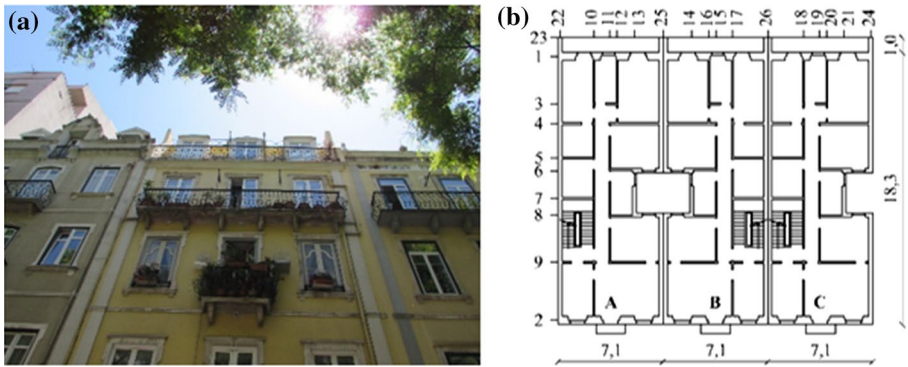
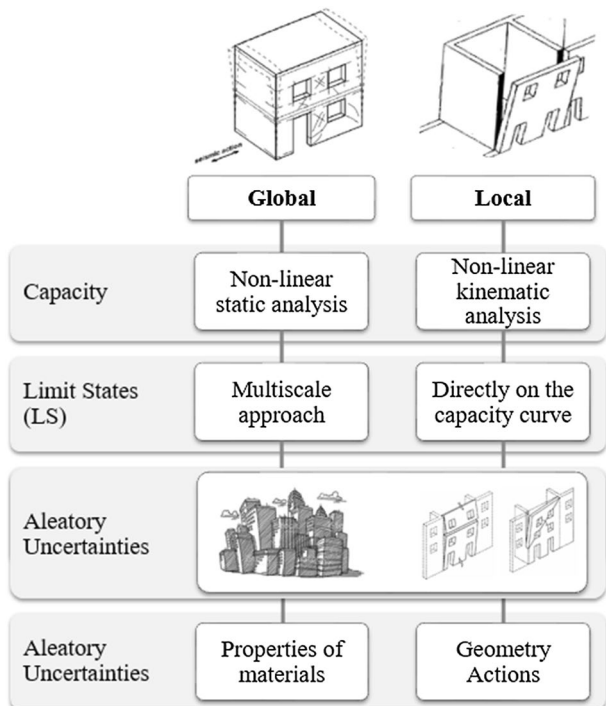


Fig. 4 Building type I: **a** exterior view of the case study, and **b** plan of the buildings A, B and C (dimensions in meters)

where d is a displacement representative of the seismic behaviour, D_{LS} is the displacement limit state threshold, Φ is the standard cumulative distribution function, IM_{LS} is the median value of the lognormal distribution of the intensity measure that produces the attainment of the limit state threshold LS, and β_{LS} is the dispersion.

As schematically represented in the flowchart from Fig. 5, to derive the fragility curves, it is proposed to perform non-linear analyses for the assessment of the in-plane and out-of-plane response of the buildings and considering the propagation of uncertainties.

Fig. 5 Assessment of the seismic performance



The assessment comprehends the comparison between the displacement capacity of the structure, identified for different performance limit states (LS), and the seismic demand, expressed by a properly reduced acceleration-displacement response spectrum. The evaluation of the corresponding seismic intensity measure is obtained from the application of the Capacity-Spectrum Method. The intensity measure (IM) adopted in this work is the peak ground acceleration (PGA), which is a common choice in case of URM buildings and justified, for the case study of this work, by the direct relation between the characteristics of the structure and the spectral characteristics of the seismic input. Despite the drawbacks, this option is possibly the most effective for a direct interpretation of results and for the comparison with other studies available in the literature.

The global seismic behaviour is addressed according to a displacement-based assessment approach (Lagomarsino and Cattari 2015) and is determined through non-linear static (pushover) analyses considering the equivalent frame model approach. Epistemic uncertainties are defined based on the logic-tree approach (Sect. 5.1.1). Different parameters are assumed as aleatory variables and treated by the Monte Carlo Method (Sect. 5.1.2). The combination between epistemic and aleatory uncertainties results in the definition a group of 1000 buildings representative of the typology. Non-linear static (pushover) analyses are performed to define the capacity of the different building models. The analyses are first carried out with the building models, defined by the median properties of the aleatory variables, in order to compare the global behaviour of the different cases of study and identify the main features and differences of the seismic response. Non-linear dynamic time-history analyses are also carried to verify the reliability of the load distributions considered in the pushover analyses. Pushover analyses are afterwards performed with the building models, defined by the aleatory properties of the various parameters.

Four performance limit states are defined on the pushover curves in terms of displacement thresholds according to the criteria proposed by (Lagomarsino and Cattari 2015) that correlates the behaviour of the structure at three scales (element, macro-element and global). The performance-based assessment comprehends the comparison between the displacement capacity of the structure, identified for different performance limit states, and the seismic demand, expressed by a reduced acceleration-displacement response spectrum (ADRS). As referred, the Capacity-Spectrum Method with over-damped spectrum is adopted in this work. The values of the seismic intensity measure compatible with the attainment of the performance limit states are treated in order to derive the parameters for the definition of the fragility functions. This includes the determination of the dispersion related to the definition of the capacity of the structure (β_C) and the dispersion related to the definition of the seismic demand (β_D). The aleatory uncertainty in the definition of β_D is related to the variability of the seismic input described by the intensity measure $0.5|\log(\text{IM}_{\text{LS},84} - \log(\text{IM}_{\text{LS},16}))|$, where $\text{IM}_{\text{LS},84}$ and $\text{IM}_{\text{LS},16}$ are the intensity measure (IM) values that produce the attainment of the limit state threshold LS by considering as input the 84% and 16% percentiles of the elastic response spectrum. Finally, the fragility functions [Eq. (1)] associated with the global seismic behaviour of the typology of buildings are derived and the damage distribution is estimated for different seismic scenarios.

The local seismic behaviour is analysed according to the displacement-based approach proposed by Lagomarsino (2015) aiming to define the seismic intensity measure compatible with specific performance limit states. The first step for the analysis comprehends the identification of the possible out-of-plane mechanisms in the URM buildings of type I. The reliability of each mechanisms is analysed as an epistemic uncertainty and treated through the logic-tree approach. In addition, as the out-of-plane behaviour is mainly related to the geometric stability rather than to the strength of materials, the geometry of the elements

and the actions involved in the mechanisms are assumed as aleatory variables. These variables are treated by a full factorial combination in order to define the input parameters for the set of mechanisms. Non-linear kinematic analyses are performed to define the capacity of the mechanisms. The performance-based assessment comprehends the comparison between the displacement capacity of the mechanisms, identified for different performance limit states, and the seismic demand, expressed by a properly reduced ADRS. As the mechanisms in this building typology are located in the upper level of the buildings, the seismic input is defined through a floor response spectrum that takes into account the dynamic filtering effect of the buildings. Moreover, in this work, the floor response spectrum is computed for each performance limit state based on an iterative procedure in order to consider the progressive damage in the building determined with the analysis of the global seismic behaviour.

The values of the seismic intensity measure compatible with the attainment of the performance limit states are treated in order to derive the parameters for the definition of the fragility functions. This includes the determination of the dispersion related to the definition of the capacity of the mechanisms based on the Response Surface Method (Liel et al. 2009), the dispersion related to the definition of the seismic demand and the dispersion related to the definition of the floor response spectrum. Finally, the fragility functions associated with the local seismic behaviour of the typology of buildings are presented and the damage distribution is estimated for different seismic scenarios.

In the end, the individual fragility curves are properly combined to define a single curve function for the class of buildings. It is proposed to first combine the global and the local seismic behaviour in each direction (for the case study only for the direction parallel to the side-walls, Y direction, is considered the local seismic behaviour) and after to adopt the minimum between the results obtained in the X and Y directions. A detailed description of the procedure for the derivation of fragility curves is presented in (Simões 2018; Simões et al. 2019a, b).

4.2 Analysis of the global behaviour

Non-linear static (pushover) analyses are carried out for both main directions (parallel and perpendicular to the façades) to assess the global seismic behaviour of the buildings. Pushover analysis is a non-linear static analysis method where the structure is subjected to constant gravity loads and monotonically varying horizontal loads aiming to simulate the effect of the seismic action on the structure (CEN 2004). The behaviour of the structure (multi-degree-of-freedom, MDOF, system) is described by the pushover curve that relates the base shear force and the horizontal displacement of a control node (assumed as representative of the structural response of the system), providing information about the stiffness, strength and displacement capacity.

For this purpose, a three-dimensional model of the group of three buildings is defined in Tremuri program (Lagomarsino et al. 2013) following the equivalent frame modelling approach (Fig. 6a). The response of the masonry panels (piers and spandrels) is modelled by non-linear beams characterized by a linear piecewise force-deformation constitutive law (Fig. 6b).

In this work, the flexural behaviour is defined according to the beam theory as proposed in Part 1 of Eurocode 8, EC8-1 (IPQ 2010) and in the Italian Code—NTC (NTC 2008). The shear behaviour of both piers and spandrels is governed by the diagonal cracking failure mode defined according to Turnšek and Čačovič (Turnšek and Čačovič 1970) and

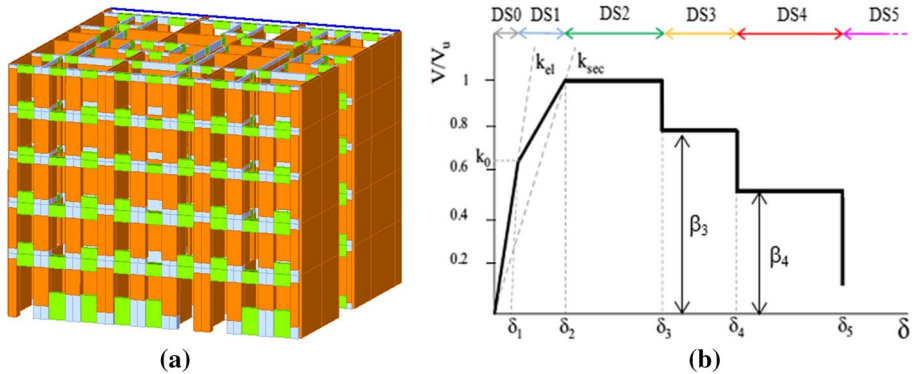


Fig. 6 **a** Model of the group of three buildings in Tremuri program and **b** force-deformation constitutive law

Turnšek and Sheppard (1980). Mixed failure modes are also possible, when the prediction between flexural and shear modes is close one to each other.

The horizontal diaphragms are modelled as membrane elements in order to consider the hypothesis of flexible diaphragms. These are defined as 3- or 4-nodes orthotropic membrane finite elements and characterized by the following equivalent parameters: thickness (t_{eq}), modulus of elasticity in the principal direction of the floor (spanning orientation, E_1 , parallel to the side-walls) and in the perpendicular direction (E_2), and shear modulus (G_{12}). In this work, the floor membrane is defined with same thickness as the floor timber boards (0.022 m) and the modulus of elasticity of the material ($E_1 = 12$ GPa). The shear modulus is defined as an aleatory variable (refer to Sect. 5.1.2) considering the difficulty in the quantification of this parameter and the reduced number of experimental testing on old timber floors.

4.2.1 Dynamic characteristics

To identify the dynamic properties of these buildings, experimental ambient vibration tests were performed in two buildings of this typology from the reference block of buildings in Lisbon. The buildings are positioned adjacent to each other (Fig. 7) and present boundary conditions that may be related to the group of three buildings considered as case of study. Therefore, the dynamic characteristics of the buildings obtained experimentally are herein compared with the dynamic characteristics of group of buildings obtained numerically.

The ambient vibration tests were carried out to each building individually. A reference accelerometer was positioned on the staircase of the buildings, while the other accelerometers were placed in different positions inside the buildings defining different tests setups. The test comprehends the determination of the modal parameters based on the response of the structure to ambient vibration forces that cannot be quantified or controlled. This type of analysis is commonly known in the literature as output-only. ARTeMIS Modal Pro (SVIBS 2013) was used for the post-processing of the data and to identify the fundamental frequencies and mode shapes of the structure identified through the amplitude peaks of the spectral density function. In order to simulate the existing boundary conditions in ARTeMIS, the four buildings identified in yellow in Fig. 7 were modelled.

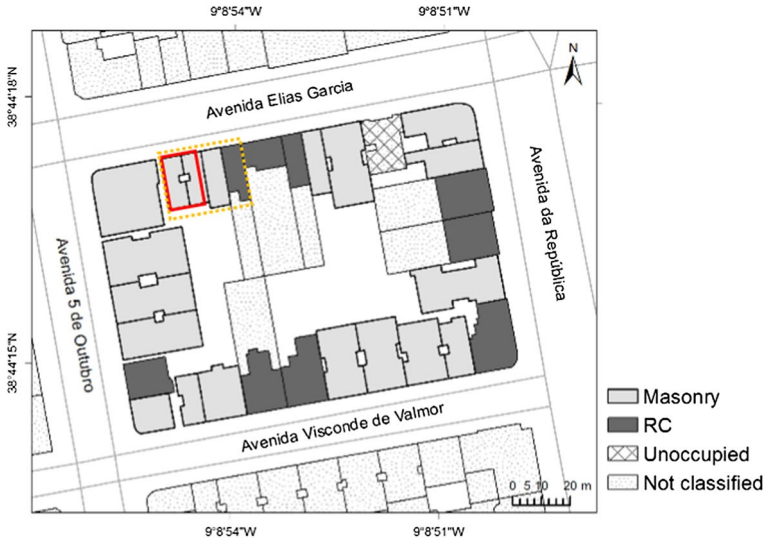


Fig. 7 Block of buildings in Lisbon (Simões et al. 2017) and identification of the tested buildings

Table 2 compares the frequencies obtained experimentally and numerically, by performing a modal analysis in Tremuri Program. The numerical model considered is characterized by the median values of the mechanical properties discussed in Sect. 5.1.2. In addition, in order to have a direct comparison between modal results, the model of the buildings was modified to incorporate the structural modifications performed to these buildings, namely the removal of internal walls and the removal of masonry piers to have large shop window on the ground floor. It should be noted that a match is obtained for the dynamic characteristics of the buildings (see last column of Table 2). Figure 8 presents, as an example, the plan view of the first mode shape in the direction of the façade walls obtained in ARTEMIS and in Tremuri Program.

Table 2 Dynamic characterization of the buildings

Mode	Mode type	Frequency (Hz)		Error	Mass participation (%)		
		Experimental	Numerical		M_x	M_y	M_z
1	Translation along Façade Walls	0.73	0.73	+ 0.0	53	0	0
2a	Translation along Side Walls	2.15	1.94	- 0.10	0	56	0
2b	Translation along Side Walls	2.34	2.08	- 0.11	0	27	0
3	Translation along Façade Walls	3.13	3.11	- 0.01	7	0	0
4	Torsion	3.61	3.42	- 0.05	0.8	0	0.1
5	Translation along Façade Walls	5.37	5.42	+ 0.01	0.9	0	0
6	Torsion	5.62	5.62	+ 0.0	0	0.4	0.1
7	Translation along Side Walls	5.99	5.58	- 0.07	0	5	0
			Average	- 0.04			

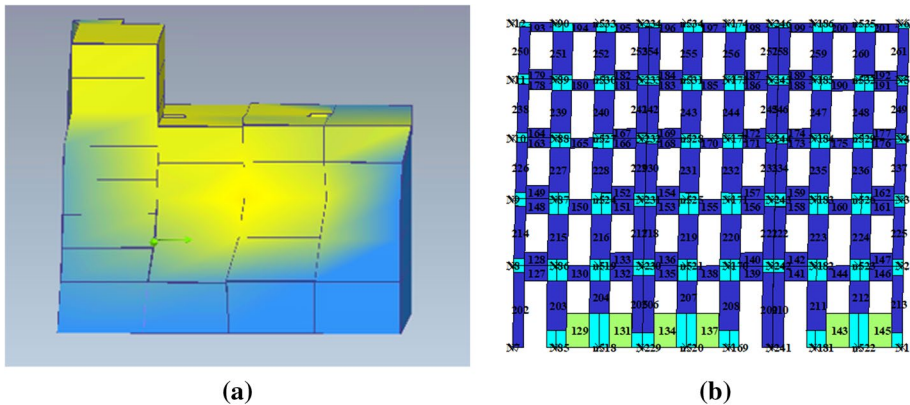


Fig. 8 First mode shape (front view) in the direction of the façade walls: **a** ARTEMIS and **b** Tremuri Program

The first fundamental mode of the buildings is along the façade walls due to the lower stiffness of the structure in this direction, particularly when in comparison with the perpendicular direction characterized by long side walls between buildings without openings. The first modes in the direction of the side walls (modes 2a and 2b) comprehend two local modes characterized by the individual mobilization of the side walls. The first torsion mode occurs with a frequency of 5.62 Hz. This type of modes is less common on this type of buildings considering that the stiffness of the structure is mainly concentrated on the exterior walls. It can also be concluded that there is a good match between experimental and numerical frequencies, validating the numerical model and indicating that the modelling assumptions considered are a good approximation of the existing condition of the buildings.

4.3 Analysis of the local behaviour

URM buildings under seismic actions are prone to local collapse mechanisms related to the out-of-plane response and overturning of façade walls insufficiently connected to the rest of the structure and standing out elements, such as gable walls, parapets and chimneys. The activation of local mechanisms depends of the quality and strength of the connections between the façade walls and elements such as side walls, partition walls, floors and roof structure.

In what concerns the URM “gaioleiro” buildings, it is reasonable to consider the collapse involving only the upper level of the façade walls, as proposed in (Simões et al. 2014b). This hypothesis is supported by: (1) the many constraints that give stability to the out-of-plane behaviour, such as, the connection to the side walls and the orientation of the timber floors perpendicular to the façade walls; and (2) experimental results from shaking table tests on reduced scale building models (Candeias 2008; Lourenço et al. 2011).

After analysing the constructive details of the last floor, three out-of-plane mechanisms are considered here (Fig. 9): the overturning of the central pier, with a plastic hinge at the base (Mech. 1), the flexural mechanism of the central pier, with a plastic hinge at the base and a plastic hinge separating the pier in two blocks (Mech. 2), and the overturning of the parapet, with a plastic hinge at the base (Mech. 3) of the parapet.

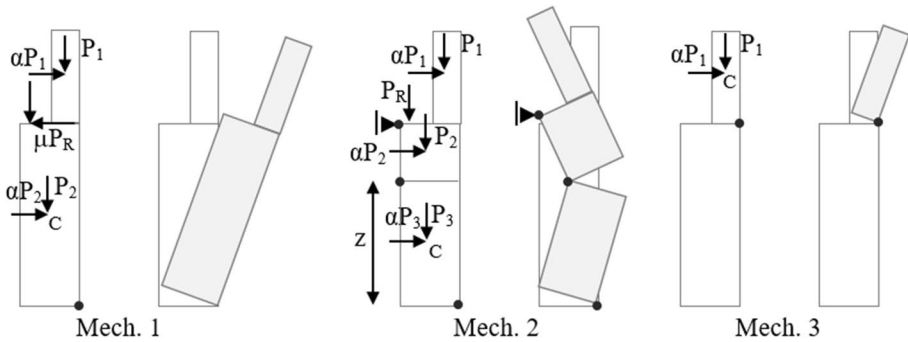


Fig. 9 Configuration and actions involved in the mechanisms: Mech. 1—overturning of the central pier, Mech. 2—flexural mechanism of the central pier and Mech. 3—overturning of the parapet

Concerning Mech. 1, the two central piers are more vulnerable to overturning than the lateral piers, as these are connected to the side walls. Assuming that the timber roof structure is connected to the interior walls and simply supported on the façade walls, in case of the overturning of the central piers, the timber elements will slide, transmitting a stabilizing horizontal force to the piers due to the friction originated in the contact surface. This force is equivalent to the vertical load transmitted by the roof to the piers (P_R) multiplied by the coefficient of friction (μ). The development of Mech. 2 is supported on the hypothesis that the horizontal displacement on top of the central piers is restrained due to the effect of strengthening, due to the insertion of tie-rods connecting the central piers to the interior walls or the introduction of a beam at the top of the wall. Then, flexural mechanism of the central piers is determinant (Griffith et al. 2004; Mendes et al. 2014). Overturning of the parapet may also occur (Mech. 3), unless these elements are fixed at the base or connect to the roof structure by steel tie-rods.

Figure 9 identifies the actions involved on the three mechanisms: P_1 , P_2 and P_3 are, respectively, the parapet and central pier self-weight, P_R is the weight of the roof transmitted to the pier, α is the coefficient proportional to the vertical loads that induces the loss of equilibrium of the system and activates the kinematism, denoted as the static seismic multiplier.

The behaviour of each local mechanism is evaluated by non-linear kinematic analyses considering the macro-block modelling approach. These analyses are based on the assessment of the work done by equilibrated forces applied to a set of compatible generalized virtual displacements (Lagomarsino 2015). The response of the mechanism is described by a curve that relates the static seismic multiplier (α) with the incremental horizontal displacement of a control node. This curve may be regarded as equivalent to the pushover curve obtained for the global seismic behaviour.

5 Evaluation of uncertainties

5.1 Global behaviour

In order to characterize the behaviour of these buildings, the main epistemic and aleatory uncertainties are briefly defined in the next sections in order to account the possible

variations within this class of buildings. The geometry of the building is not considered an uncertainty as the layout of the buildings is similar.

5.1.1 Epistemic uncertainties

The epistemic uncertainties for the analysis of the global behaviour are related to the incomplete knowledge about the structure of the buildings. Different classes of buildings have been identified in previous works about the URM “gaioleiro” buildings in Lisbon (Simões et al. 2018; Simões 2018). These classes account for variations at:

- Ground floor configuration: use of the building as i) housing (H) or as ii) shop (S).
- Constructive details: (1) side walls shared between adjacent buildings (S) or (2) independent (I).
- Side walls material: (1) solid clay brick masonry (S) or (2) solid clay brick masonry in the first two floors and hollow clay brick masonry in the last three floors (SH).
- Main interior walls material: (1) solid clay brick masonry (S), (2) solid clay brick masonry in the first two floors and hollow clay brick masonry in the last three floors (SH), or (3) solid clay brick masonry in the first two floors, hollow clay brick masonry in the intermediate floors and timber walls on the last floor (T).
- Partition walls material: (1) hollow brick masonry (H) or (2) timber walls (T).

These features are treated by the logic-tree approach. A probability is attributed to each feature based on the information available in the literature and on a detailed survey to existing block of buildings (Simões et al. 2017). This aims to define different prototypes representative of the URM buildings constructed in Lisbon in the early twentieth century.

The different values adopted for the probability of each feature are defined in Fig. 10 and explained in the following. In what concerns the ground floor configuration, 33% of the buildings from the referred block of buildings are used for housing, while 67% are used for shopping. This has implications on the layout of the rooms and openings at the ground floor level. In the reference block of buildings, 33% of the buildings have shared side walls and 67% have independent side walls. The decision may depend on the time of construction (and the presence of adjacent buildings) and on the dimension of the lot.

There is limited information about the materials used on the construction of these buildings. The exterior walls were constructed in rubble stone masonry on the street and rear façade walls and clay brick masonry on the side walls. Brick units may be: i) solid in all floors or ii) solid in the lower floors and hollow in the upper floors. The Building Regulation from 1930 (RGEUL 1930) recommended to use hollow bricks only in the last two floors of the side walls. Considering that this regulation was published in the end of the construction period of these buildings, a lower probability is attributed to this option. Therefore, it is assumed that the side walls of 70% of the buildings are made of solid clay brick masonry, while the remaining 30% are made of solid clay brick masonry in the first three floors and hollow clay brick masonry in the last two floors. It is estimated that the main interior walls are made of solid clay brick masonry in 50% of the buildings while they are made of solid clay brick masonry in the ground floor and hollow clay brick masonry in the other floors in 50% of the buildings. However, there are records of buildings in which the majority of the interior walls are made with timber structure. In order to consider also this option, in 20% of the buildings the main interior walls are assumed to be made of timber (but limiting them to the last floor of the buildings, as indicated in (RGEUL 1930)) and

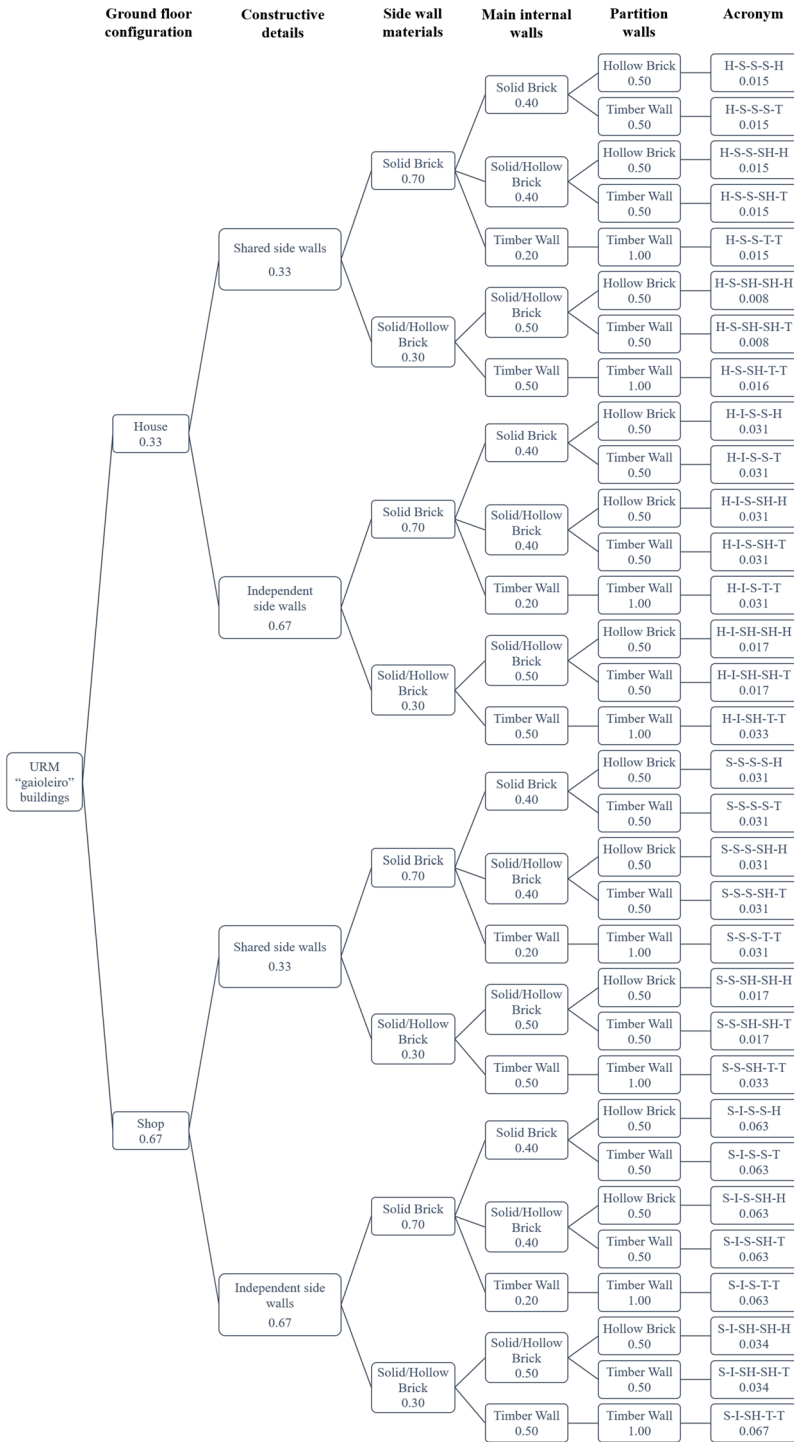


Fig. 10 Logic-tree for URM “gaioleiro” buildings

to reduce the previous probabilities associated to clay brick masonry to 40/40. As to the partition walls, it is estimated that in 50% of the buildings these are made of hollow clay brick masonry, while in 50% of the buildings these are made of timber structure.

Figure 10 presents the logic-tree for the URM “gaioleiro” buildings in Lisbon. The end of a branch of the tree represents a class of buildings with specific features, identified by an acronym. The probability attributed to the class of buildings is determined by multiplying the probability of all the component branches of the tree. A total of 32 building classes are considered.

As an example, Fig. 11 shows the pushover curves obtained for the first eight branches of the logic-tree, for both X and Y directions.

5.1.2 Aleatory uncertainties

Aleatory uncertainties are related with the randomness of a certain phenomenon. For the analysis of the global behaviour, the aleatory variables account for variations on the mechanical properties of masonry, strength and deformability characteristics of masonry piers and spandrels, mechanical properties of interior timber walls, quality of connections between walls and in-plane stiffness of timber floors.

It is proposed to treat these aleatory variables by the Monte Carlo Method (Rubinstein 2011) in order to define, in a random way, the properties to be assigned to the numerical models. A total of 1000 simulations are considered in order to have a sufficient number of results (from a statistical point of view) to reach a good convergence in the estimation of the dispersion of the capacity for the global behaviour (β_C).

To do so, first, for each aleatory variable (X_k), a plausible range of variation is defined based on reference values available in literature and codes. Second, an appropriate distribution of probability is attributed and characterized by median value (X_{med}) and dispersion (β) so that the 16% and 84% percentiles of the distribution correspond, respectively, to the lower and upper values of the range of variation. An alternative procedure to the 16% and 84% percentiles is to consider the coefficient of variation, as suggested in the Probabilistic Model Code (Joint Committee on Structural Safety 2011). Lognormal distributions were attributed to the aleatory variables varying between $]0, +\infty[$ and beta distributions for those varying between $[0, 1]$ or having, from a physical point of view, a range of variation equal to one. A total of 50 aleatory variables are considered and divided in 17 groups (Table 3).

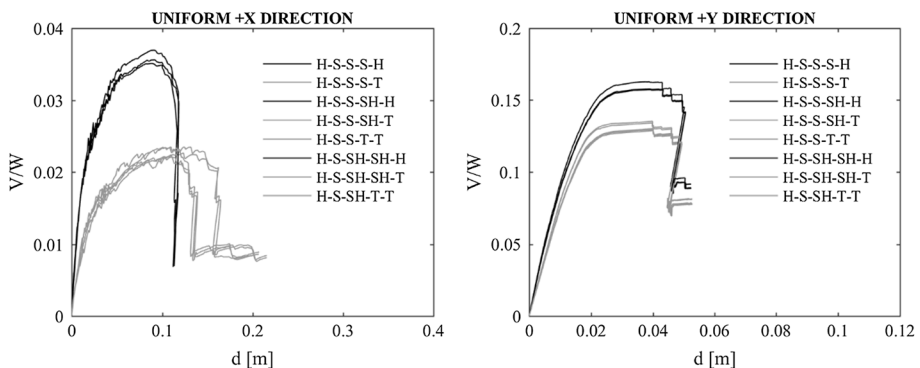


Fig. 11 Pushover curves for the first the group of buildings (H-S): X direction (left) and Y direction (right)

Table 3 Characterization of aleatory variables

Description	Group	X_k	Distribution	X_{med}	β
Rubble stone masonry	1	$E-G-f_m$ (MPa)	Lognormal	736.50–245.50–0.95	0.18–0.18–0.12
	2	τ_0 (MPa)	Lognormal	0.022	0.18
Solid brick masonry	3	$E-G-f_m$ (MPa)	Lognormal	840.65–280.22–1.07	0.16–0.16–0.11
	4	τ_0 (MPa)	Lognormal	0.074	0.21
Hollow brick masonry	5	μ_{loc}	Lognormal	0.53	0.28
	6	$E-G-f_m$ (MPa)	Lognormal	840.65–280.22–0.87	0.16–0.16–0.14
	7	τ_0 (MPa)	Lognormal	0.074	0.21
	8	μ_{loc}	Lognormal	0.53	0.28
Spandrels in façade walls	9	$E-G-f_m$ (MPa)	Lognormal	779.10–259.70–1.00	0.24–0.24–0.17
	10	τ_0 (MPa)	Lognormal	0.041	0.82
Drift thresholds for piers	11	$Int-\mu_{loc}$	Lognormal	1.00–0.53	0.69–0.28
	12	$\delta_{F3}-\delta_{F4}-\delta_{F5}$	Lognormal	0.0058–0.0098–0.0147	0.24–0.22–0.20
		$\delta_{S3}-\delta_{S4}-\delta_{S5}$	Lognormal	0.0029–0.0049–0.0069	0.24–0.22–0.20
	Drift thresholds for spandrels	13	$\beta_{F4}-\beta_{S3}-\beta_{S4}$	Beta	0.85–0.70–0.40
$\delta_{F3}-\delta_{F4}-\delta_{F5}$			Lognormal	0.0019–0.0058–0.0194	0.24–0.25–0.25
$\delta_{S3}-\delta_{S4}-\delta_{S5}$		Lognormal	0.0019–0.0058–0.0194	0.24–0.25–0.25	
$\beta_{F4}-\beta_{S3}-\beta_{S4}$		Beta	0.55–0.55–0.55	0.15–0.15–0.15	
Stiffness degradation of masonry panels	14	$\beta_{F4}-\beta_{S3}-\beta_{S4}$ llfaç	Beta	0.40–0.40–0.40	0.20–0.20–0.20
		μ llfaç	Beta	4.20	0.99
Timber walls	15	$k_{in}-k_0$	Beta	0.65–0.50	0.15–0.25
		$E-G-f_m$ (MPa)	Lognormal	109.54–1.73–0.54	0.60–0.55–0.29
Link beams	16	$A-I$ (m ² –m ⁴)	Lognormal	0.0004–0.0002	0.81–0.81
		G (MPa)	Lognormal	9.88	0.48

E , modulus of elasticity; G , shear modulus; f_c , compressive strength; τ_0 , equivalent shear strength; μ_{loc} , coefficient of friction on the mortar joints in the end section of spandrels; Int , interlocking of the masonry units in the end section of spandrels; δ_{S3} , drift limit for the shear behaviour at damage level i; δ_{F3} , drift limit for the flexural behaviour at damage level i; β_{S3} , residual strength for the shear behaviour at damage level i; β_{F3} , residual strength for the flexural behaviour at damage level i; μ , ductility of the brick arch for damage level 3; k_{in} , ratio between the initial (k_{e1}) and the secant (k_{sec}) stiffness (Fig. 6b); k_0 , ratio between the shear force at the end of the elastic phase and V_u (Fig. 6b); A , area of the link beams and I , inertia of the link beams

Within each group, the variables are fully correlated assuming that their variation is identical in each model.

The range of values for Group 1 and 2 (rubble stone masonry), Group 3 and 4 (solid brick masonry) and Group 6 and 7 (hollow brick masonry) are defined from the application of the Bayes Theorem as presented in Sect. 3.2.

Group 5, 8 and 11 refer to the modelling of the flexural behaviour of spandrels according to the criterion proposed in Cattari and Lagomarsino (2008) assuming an equivalent tensile strength on the elements due to the interlocking of the masonry units at the end section of spandrels (Int —ratio between length and height of the masonry unit). For brick masonry, Int is equal to 2 (deterministic value). For rubble stone masonry, lower values are expected due to the masonry irregularity (Group 11). Another input is the coefficient of friction in the mortar joints in the end section of spandrels (μ_{loc} —Group 5, 8 and 11).

Groups 9 and 10 characterize the mechanical properties of spandrels in the façade walls. Considering that these panels may be made of rubble stone masonry or clay brick masonry, the properties attributed, range between the mechanical properties of the two types of materials.

Groups 12, 13 and 14 are related to the formulation of the linear piecewise constitutive law associated with the initial stiffness degradation (k_{in} and k_0) and the progressive degradation of strength (δ_i and β_i) of the panels.

The values for Groups 12 and 13 are defined based on experimental test results (Kržan et al. 2015; Vanin et al. 2017) and expert judgement. For instance, in case of piers, the ultimate drift levels (DL4) reflect the recommendations from structural codes (IPQ 2017; NTC 2008): between 0.4 and 0.6% in case of shear failure and between 0.8 and 1.2% in case of flexural failure. In case of spandrels, the experimental results from (Beyer and Mangalathu 2014) are taken into account to characterize the behaviour of the shallow brick arches present in the façade walls and of the timber elements in the clay brick masonry walls. For spandrels with shallow brick arches, DL3 threshold is not defined in terms of drift, but in terms of ductility (μ), considering the greater deformation capacity of the elements observed during the experimental tests (Beyer and Mangalathu 2014). Due to the limited information available, the same intervals of values are adopted for the different types of masonry. It is noted that recent results in literature suggest lower drift values (Morandi et al. 2018), nevertheless refers to modern hollow bricks, which are more fragile than older hollow bricks in Gaioleiro buildings, which present a lower percentage of hollows.

In what concerns Group 14, structural codes (IPQ 2010; NTC 2008) recommend to adopt a 50% reduction of the elastic stiffness properties (corresponding to $k_{in}=2$), unless more detailed information is available. Previous parametrical studies have indicated this level of reduction leads to conservative estimate of the non-linear behaviour of the panels (Cattari and Lagomarsino 2013). Therefore, it is proposed to vary k_{in} between 1.00 and 1.50, in order to simulate the extreme cases in which there is no stiffness degradation and the case in which this reduction is approximately 67% due to the expected cracked state of the buildings. As to k_0 , it is proposed to consider a range between 0.50 and 0.80.

Group 15 quantifies the mechanical properties of the interior timber walls. The mechanical properties of these walls are determined based on the experimental results from compression and shear tests performed by (Rebelo et al. 2015). Group 16 defines the area (A) and inertia (I) of the link beams that set the connection between perpendicular exterior walls. These connections are defined as medium quality connections justified by the use of different materials between façade walls (rubble stone masonry) and side walls (brick masonry). The connection between exterior walls and interior clay brick masonry walls are defined as weak quality connections taking into account that the interior walls were constructed after

exterior walls. The properties of the link beams representative of the weak quality connections are assumed as deterministic. Group 17 characterizes the flexible behaviour of timber floors, represented by the shear modulus (G) of an equivalent finite membrane element with 0.022 m of thickness, corresponding to the thickness of the timber boards. The range of variation is defined in (NZSEE 2017), which proposes reference values as a function of the floor system and state of conservation, based on Giongo et al. (2013).

The Monte Carlo simulations are defined for each variable starting from the continuous probability density function attributed and considering additional correlations between variables, as described in the following. It is assumed that within the 17 groups, the aleatory variables are fully correlated in order to guarantee a positive linear relationship between the variables attributed to the same model (correlation coefficient, $R = +1$). A negative linear correlation ($R = -1$) is considered for Group 14 related to the initial stiffness degradation of the masonry panels. This aims to define two extreme behaviours for the transition between elastic and plastic phases. Thus, for higher initial stiffness degradation (higher value of k_{in}) a lower value of k_0 is expected, so to have a longer interval between the first cracks and the reaching of the ultimate strength capacity (the opposite relation is also valid). It is also proposed to assume a correlation coefficient of 0.5 between Group 1 and 2, Group 3 and 4, Group 6 and 7 and Group 9 and 10, taking into account that the modulus of elasticity (E), the shear modulus (G) and the compressive strength (f_c) are not fully correlated nor uncorrelated with the equivalent shear strength (τ_0).

5.2 Local behaviour

The reliability of each local mechanism is analysed as an epistemic uncertainty, while the geometry of the elements and the actions involved in the mechanisms are assumed as aleatory variables. The involved uncertainties are described in the next sections.

5.2.1 Epistemic uncertainties

The occurrence of collapse mechanisms depends on the condition of the building and possible strengthening interventions to prevent the overturning of the central piers and parapets. In this regard, the local behaviour of the buildings may be analysed by considering two different scenarios:

1. The last floor of the buildings, with the hypothesis of: (1) overturning of the central piers (Mech. 1) or (2) flexural mechanism of the central piers (Mech. 2).
2. The parapet, with the hypothesis of: (1) overturning (Mech. 3) or (2) no overturning, in case strengthening has been implemented or the building has no parapet.

Each scenario is assumed as an epistemic uncertainty and again treated by the logic-tree approach, as presented in Fig. 12. An expert judgement probability is attributed to each branch of the tree. In what concerns the first scenario, a lower probability is defined for Mech. 2 considering that the flexural mechanism only occurs in case a strengthening solution has been implemented. Thus, it is assumed that in 70% of the cases Mech. 1 may occur. In what concerns the second scenario, it is assumed that in 60% of the cases Mech. 3 may occur. It is noted that the overturning of the parapet to the street is relevant from the point of view of life safety, however from the point of view of the performance limit state of the main building, it addresses a non-structural element.

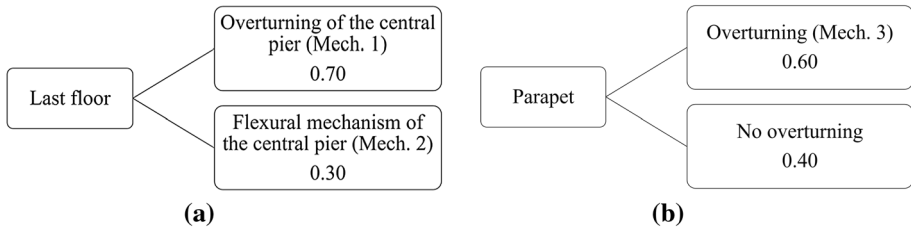


Fig. 12 Local behaviour scenarios: **a** last floor of the building and **b** parapet

5.2.2 Aleatory uncertainties

The aleatory variables for the analysis of the local behaviour account for the geometry of the blocks involved in the mechanisms and the value of the external forces applied. Although the geometry of the building is considered deterministic, for the analysis of the local behaviour, the thickness of the parapet ($t_{parapet}$) and the thickness of the central pier (t_{pier}) are considered aleatory variables as the behaviour of the mechanisms is mainly influenced by the geometry of the blocks. The external forces applied comprehend the weight of the roof transmitted to the pier (P_R) and the equivalent horizontal force (μP_R), i.e. the self-weight of the roof (γ_R) and the coefficient of friction (μ) are considered as aleatory variables.

The aleatory variables are treated by the Response Surface Method. Each aleatory variable is described by a lower ($X_{k,low}$), median ($X_{k,med}$) and upper ($X_{k,up}$) values. This method is based on the approximation of the hyperplane that fits the response surface of the variable $\log(IM_{LS})$ in the hyperspace of the normalized variables representing the aleatory variables considered. The angular coefficients (β_{Ci}) defining the hyperplane are determined according to:

$$\beta_{Ci} = (Z^T Z)^{-1} Z^T Y \tag{2}$$

where Z is a matrix, with M rows \times N columns ($M = 2^N$ is the number of models defined by the full factorial combination and N is the number of aleatory variables), which collects the corresponding normalized variables (equal to -1 for $X_{k,low}$ and $+1$ for $X_{k,up}$) and Y is a vector, with M rows, which collects the corresponding $\log(IM_{LS})$ values. The dispersion in the definition of the capacity of the local mechanism (β_C) is given by:

$$\beta_C = \sqrt{\beta_{Ci}^T \beta_{Ci}} \tag{3}$$

The values of the aleatory variables considered ($X_{k,low}$, $X_{k,med}$ and $X_{k,up}$, respectively) are summarized in Table 4.

Table 4 Characterization of the aleatory variables in terms of lower, median and upper values

X_k	$X_{k,low}$	$X_{k,med}$	$X_{k,up}$
$t_{parapet}$ (m)	0.10	0.13	0.15
t_{pier} (m)	0.35	0.38	0.40
γ_R (kN/m ²)	0.88	1.09	1.30
μ (-)	0.40	0.50	0.60

Table 5 Combination of aleatory variables for each mechanism

Mech.	Variables X_k	N	$Q=2^N$
1	$t_{parapet}, t_{pier}, \gamma_R, \mu$	4	16
2	$t_{parapet}, t_{pier}, \gamma_R$	3	8
3	$t_{parapet}$	1	2

Table 6 Resulting parameters of fragility curves for the URM buildings

PL	Action type 1		Action type 2	
	$PGA_{50\%}$ (m/s ²)	β	$PGA_{50\%}$ (m/s ²)	β
1	0.341	0.406	0.816	0.447
2	0.631	0.354	1.489	0.407
3	1.289	0.317	2.805	0.308
4	1.447	0.325	3.050	0.288

In the global model of the buildings, the street façade in the last floor is defined with 0.40 m of thickness. Considering that the thickness of the façade walls decreases along the height, approximately 0.05 m in each floor, the same variation is now assumed for the thickness of the central pier (t_{pier}). In addition, in the global model of the buildings, the parapet is defined with 0.15 m of thickness and 0.80 m of height. In this case, the thickness of the parapet ($t_{parapet}$) is considered between 0.10 and 0.15 m. The self-weight of the roof (γ_R) is defined by the interval of values proposed by (Ferreira and Farinha 1974). The coefficient of friction (μ) between timber and masonry is defined from (Farinha and Reis 1993; Zhang et al. 2008).

The aleatory variables are treated by a full factorial combination at two levels. For each of the $Q=2^N$ models, the aleatory variables assume the values correspondent to the lower ($X_{k,low}$) and upper ($X_{k,up}$) values of the interval. Table 5 identifies the variables involved in the three out-of-plane mechanisms and the number of combinations/models considered for the analysis of the local seismic behaviour.

6 Fragility analysis

6.1 Derivation of fragility curves

The fragility curves for these buildings result from the combination of the fragility curves obtained for the global and local behaviour and after considering the contribution of the different classes of buildings identified by the global logic-tree in Fig. 10 (for additional information refer to (Simões et al. 2019a, b)). In this work, it is proposed to add the contribution of PLk at the local scale ($P_{L,PLK}$) to the corresponding PLk at the global scale ($P_{G,PLK}$) according Eq. (4).

$$P_{PLK} = P_{G,PLK} + (1 - P_{G,PLK})P_{L,PLK} \tag{4}$$

Table 6 summarizes the parameters for the fragility curves considering the global seismic behaviour of the typology for the two seismic actions of the applicable code in Lisbon (IPQ 2010) and Fig. 13 plots the corresponding functions for seismic action type 1

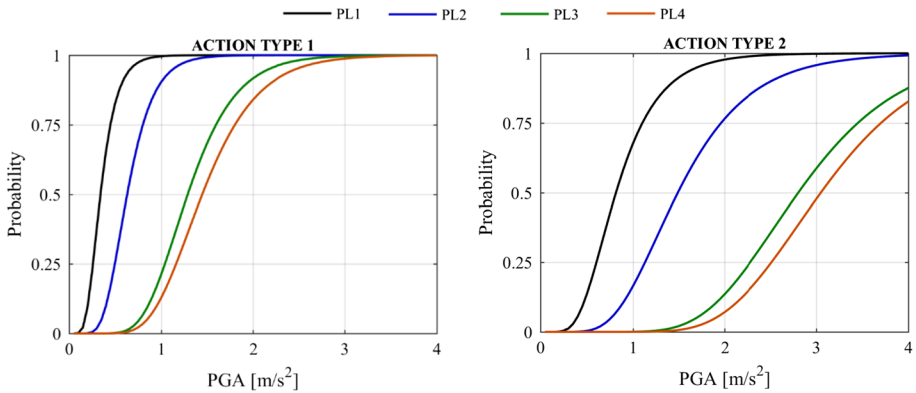
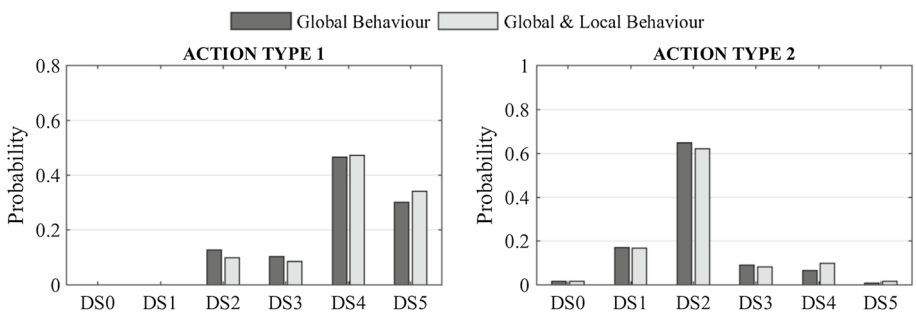


Fig. 13 Fragility curves for the URM buildings: seismic action type 1 (left) and type 2 (right)

and type 2 progressing four damage levels assumed to correspond to the EMS98 scale (Grünthal 1998). These fragility curves consider the different sources of uncertainties that influence the seismic performance of the buildings, providing the overall assessment of the seismic vulnerability of this class of buildings.

The discrete probability associated with the different damage states is determined following the procedure presented in (Lagomarsino and Cattari 2014). The damage states (DS_k with $k=1, \dots, 5$) are defined to be conceptually compatible with the European Macroseismic Scale (EMS-98 (Grünthal 1998)): DS₀—no damage, DS₁—slight damage, DS₂—moderate damage, DS₃—heavy damage, DS₄—very heavy damage, and DS₅—collapse. Figure 14 shows the corresponding probability damage distribution considering the code seismic actions for Lisbon (IPQ 2010) for a return period of 475 years are



Distribution of damage		DS0	DS1	DS2	DS3	DS4	DS5
Action Type 1 PGA = 1.94 m/s ²	Global Behaviour	0.000	0.001	0.128	0.104	0.467	0.301
	Global & Local Behaviour	0.000	0.001	0.099	0.085	0.474	0.341
Action Type 2 PGA = 2.16 m/s ²	Global Behaviour	0.015	0.171	0.649	0.089	0.066	0.009
	Global & Local Behaviour	0.015	0.167	0.622	0.082	0.099	0.015

Fig. 14 Distribution of damage for the URM buildings for seismic action type 1 (PGA = 1.94 m/s²) and type 2 (PGA = 2.16 m/s²)

considered for the estimation of the damage distribution: type 1 ($PGA = 1.94 \text{ m/s}^2$) and type 2 ($PGA = 2.16 \text{ m/s}^2$).

It is estimated that there is about 47% probability of having very heavy damage (DS4) and about 34% probability of collapse (DS5). As expected, the contribution of the local seismic behaviour increased the final vulnerability for the higher damage states. These outcomes, put in evidence the high seismic vulnerability of these URM buildings and the urgent need to reduce potential losses due to future earthquakes.

6.2 Comparison with other fragility curves

Fragility curves available in the literature addressed to URM buildings such as the ones in Lisbon are scarce. The comparison of fragility curves defined for traditional masonry located in different regions is also questionable as the seismic vulnerability depends on the local materials and on the local seismic culture. Therefore, in this section, the fragility curves proposed for the URM buildings are compared with the fragility curves derived in previous studies about these buildings (Simões et al. 2014a, 2015). In addition, the method proposed by Vicente et al. (2011) for the vulnerability assessment of masonry buildings is applied to the present case in order to derive the corresponding fragility curves. Final reference is made to the fragility curves proposed by D’Ayala et al. (1997) for the URM buildings located in Alfama, one of the oldest districts in Lisbon.

In Simões et al. (2014a, 2015) the fragility curves for these buildings were determined based on non-linear static (pushover) analyses and considering only the global seismic behaviour. The fragility curves were defined by assuming a lognormal cumulative distribution and some conventional values for the dispersion (β) of the different performance limit states (also in terms of PLk, with $k = 1, \dots, 4$). In this case, the dispersion accounted for the uncertainties in the definition of the capacity (β_c) of buildings, seismic demand (β_D), limit states (β_T) and the error associated with the model used for the analysis (β_e). Figure 15a compares the fragility curves in question for seismic action type 1 (the most demanding case). It is observed that the curves previously defined are closer to each other, whereas

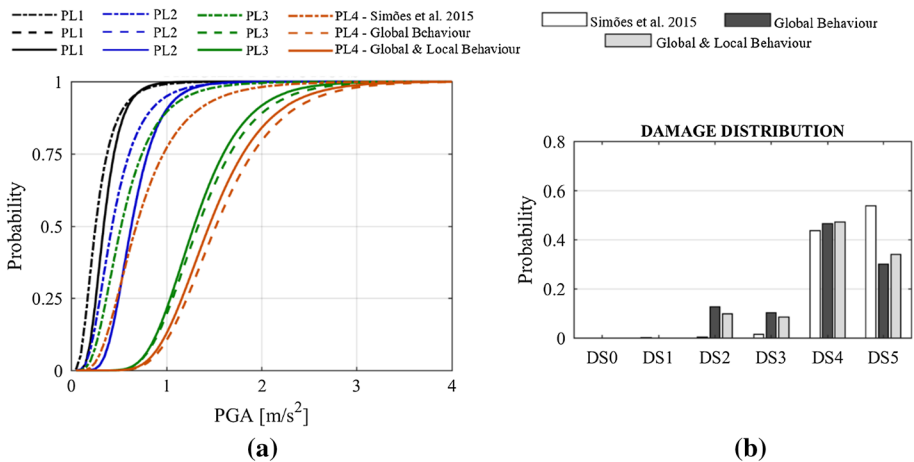


Fig. 15 Comparison of the results obtained in Simões et al. (2015) and in the present work: **a** fragility curves and **b** distribution of damage for action type 1— $PGA = 1.94 \text{ m/s}^2$

the curves now proposed for PL2 to PL4 are shifted to the right side of the plot. Figure 15b compares the probability damage distribution for the code seismic action for Lisbon. The probabilities associated with the lower damage states increased with the new fragility curves, when the contribution of the local seismic behaviour is considered, whereas the probability of collapse (DS5) decreased from 54 to 30%.

The hybrid method developed by Vicente et al. (2011) was also applied here. The method combines the empirical vulnerability index formulation suggested by the GNDT II level approach (GNDT 1994), including some modifications, with the Macroseismic Vulnerability Model defined by Lagomarsino and Giovinazzi (2006). Figure 16a compares the fragility curves obtained from the application of the method proposed by Vicente et al. (2011), dashed lines, and the curves proposed in this work, considering both the global and local behaviour, solid lines. This option is consistent with the method proposed by Vicente et al. (2011) as it takes into account both the global and local seismic behaviour of the buildings. Figure 16b compares the results in terms of the probability damage distribution for $PGA = 1.94 \text{ m/s}^2$, showing that the probability of having heavy damage (DS4) and the probability of collapse (DS5) estimated by the hybrid method are lower than the proposed in this work: 38% in contrast with 47% for DS4, and 19% in contrast with 34% for DS5.

D’Ayala et al. (1997) analysed 200 URM buildings in Alfama district, in Lisbon, with 2 to 6 storeys. These buildings were constructed before the 1755 earthquake and have been subjected to several repairs and modifications afterwards. The vulnerability assessment was supported on the application of a simplified limit-state approach (analytical method). The fragility functions proposed by D’Ayala et al. (1997) consider as performance limit states the damage scale from the European Macroseismic Scale (EMS-98). Here a direct correspondence between PLk and the DSk is considered. Figure 17a compares the fragility functions proposed by D’Ayala et al. (1997), dashed lines, and the new fragility functions. The curves are quite diverse and indicate that the URM buildings constructed in Alfama are less vulnerable than the URM buildings constructed in the transition between the nineteenth and twentieth centuries in Lisbon. Figure 17b compares the results in terms of the probability damage distribution for $PGA = 1.94 \text{ m/s}^2$.

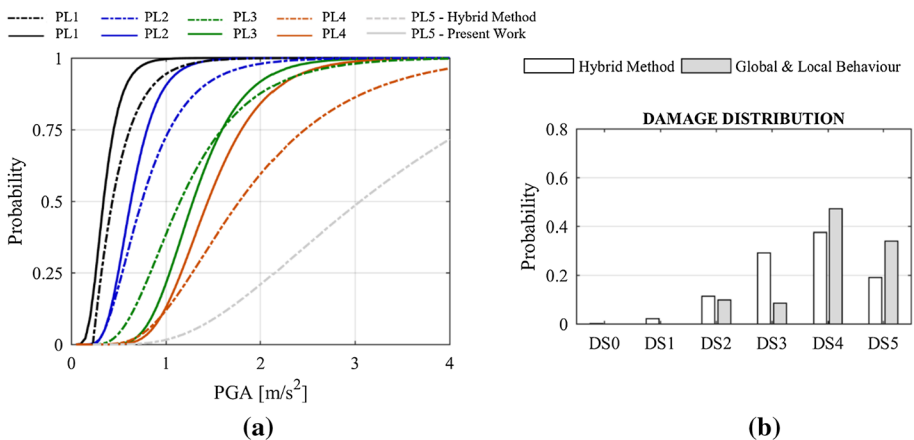


Fig. 16 Comparison of the results obtained with the hybrid method and in the present work: **a** fragility curves (discontinuous—hybrid method and solid lines—present work) and **b** distribution of damage for action type 1— $PGA = 1.94 \text{ m/s}^2$

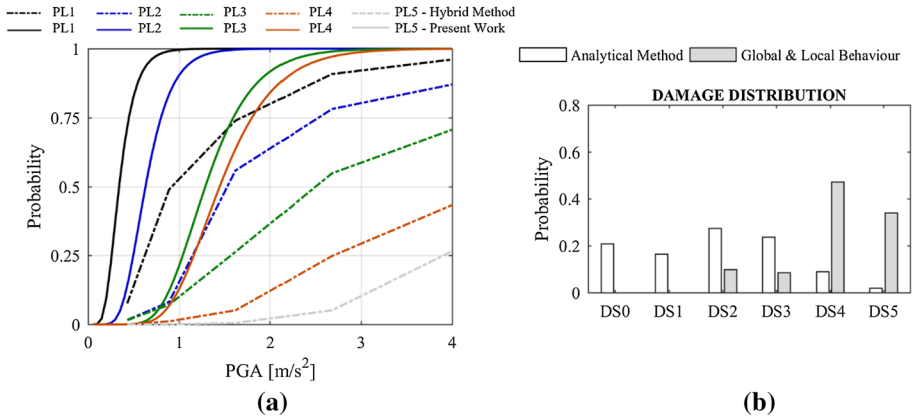


Fig. 17 Comparison of the results obtained in D’Ayala et al. (1997) and in the present work: **a** fragility curves (discontinuous lines—D’Ayala et al. (1997) and solid lines—present work) and **b** distribution of damage for action type 1—PGA = 1.94 m/s²

The comparison of the fragility curves and the corresponding distribution of damage for the code seismic action type 1 for Lisbon (PGA = 1.94 m/s²) indicated that the vulnerability estimated in the present work is between the results obtained from previous works, supported on a simplified approach (only one building was analysed) and conventional parameters, and the results obtained from the application of the hybrid method proposed by Vicente et al. (2011). The curves proposed by D’Ayala et al. (1997) indicated that older URM buildings in Lisbon are less vulnerable than the more recent and taller URM buildings; indeed, it is worth noting that buildings in Alfama district survived to the 1755 Lisbon earthquake (even if with some damage), while the vulnerability of Gaioleiro buildings is well evident. Table 7 compares, in addition, the dispersion of the different fragility curves for different PLi. The curves proposed in this work have lower values of dispersion. This may be justified by the fact that in the previous methods the dispersion was based on conventional values, that are related to a typology in which buildings of different configurations are present (e.g. aggregated buildings in the Alfama district); on the contrary, the typology analysed in the present work is made by a well-defined configuration and, in addition, the different contributions for the total dispersion have been determined in a more detailed.

Table 7 Comparison of the dispersion

PL	This work	Simões et al. (2015)	Hybrid method Vicente et al. (2011)	D’Ayala et al. (1997)
1	0.406	0.575	0.477	0.730
2	0.354	0.518	0.478	0.629
3	0.317	0.517	0.471	0.805
4	0.325	0.517	0.478	0.705
5	–	–	0.475	0.584

7 Final remarks

The article addresses the seismic vulnerability assessment of a typology of URM buildings constructed in Lisbon between the nineteenth and the twentieth centuries. The assessment includes the generation of fragility curves that combine the in-plane and out-of-plane response following different criteria and methods of analysis. The fragility curves are derived considering the propagation of both epistemic and aleatory uncertainties on the analysis. Among different alternatives (e.g. artificial neural networks or machine learning methods), in this paper the epistemic uncertainties have been treated by the logic-tree approach, through the definition of different classes of buildings representative of the typology. The aleatory uncertainties were treated by the Monte Carlo Method in case of the global seismic behaviour and of the Response Surface Method in case of the local seismic behaviour. The first method requires a larger number of analyses to obtain a reliable outcome, while the second method needs only a few points to define the hyperplane that fits the response surface of the variables. Notwithstanding the lower computational burden, the application of the Response Surface Method to the analysis of the global seismic behaviour would not be feasible for the comprehensive analyses of the variations within a typology of buildings.

The final fragility curves, providing the overall assessment of the seismic vulnerability of this class of buildings, were evaluated. These curves combine the fragility curves obtained for the global and local behaviour. The results put in evidence the seismic vulnerability of this class of URM buildings. For instance, considering the earthquake-resistant code for Lisbon with a return period of 475 years, it was estimated about 50% probability of having heavy damage and about 30% probability of collapse. The structural intervention on these buildings is urgent in order to reduce potential losses due to future earthquakes. Similar results were obtained, between global and local behavior, as the vulnerability of this typology is mainly controlled by the in-plane behavior of the masonry walls. As expected, the contribution of the local seismic behaviour increased the final vulnerability for the higher damage states.

Acknowledgements The first author would like to acknowledge the financial support of *Fundação para a Ciência e a Tecnologia* (FCT, *Ministério da Educação e Ciência*, Portugal) through the scholarship PD/BD/106076/2015 through the FCT Doctoral Program: Analysis and Mitigation of Risks in Infrastructures, INFRARISK- (<http://infrarisk.tecnico.ulisboa.pt>). The authors would also like to acknowledge the contribution from Bruno Silva (Instituto Superior Técnico) and Nuno Mendes (University of Minho) regarding the ambient vibration tests.

References

- Appleton JG (2005) Reabilitação de Edifícios “Gaioleiros”, 1st edn. Edições Orion, Lisboa (in Portuguese)
- Beyer K, Mangalathu S (2014) Numerical study on the peak strength of masonry spandrels with arches. *J Earthq Eng* 18:169–186. <https://doi.org/10.1080/13632469.2013.851047>
- Bracchi S, Rota M, Magenes G, Penna A (2016) Seismic assessment of masonry buildings accounting for limited knowledge on materials by bayesian updating. *Bull Earthq Eng* 14(8):2273–2297. <https://doi.org/10.1007/s10518-016-9905-8>
- Candeias P (2008) Avaliação Da Vulnerabilidade Sísmica de Edifícios de Alvenaria. Ph.D. Thesis. Universidade do Minho. Guimarães (in Portuguese)
- Cattari S, Lagomarsino S (2008) A strength criterion for the flexural behaviour of spandrels in un-reinforced masonry walls. In Proceedings of the 14th earthquake conference on earthquake engineering, Beijing
- Cattari S, Lagomarsino S (2013) Seismic assessment of mixed masonry-reinforced concrete buildings by non-linear static analyses. *Earthq Struct* 4(3):241–264. <https://doi.org/10.12989/eas.2013.4.3.241>

- CEN (2004) Eurocode 8: Design of structures for earthquake resistance. Part 1: general rules, seismic actions and rules for buildings Eurocode, EN 1998-1. European Committee for Standardization (CEN), Brussels
- D'Ayala D, Spence R, Oliveira CS, Pomonis A (1997) Earthquake loss estimation for Europe's historic town centres. *Earthq Spectra* 13(4):773–793
- Farinha J, Reis A (1993) Tabelas Técnicas, 2nd edn. Edição P.O.B, Setúbal (**In Portuguese**)
- Ferreira V, Farinha J (1974) Tabelas Técnicas Para Engenharia Civil, 7th edn. Técnica. Associação de Estudantes do Instituto Superior Técnico, Lisboa (**in Portuguese**)
- Franchin P, Pagnoni T (2018) A general model of resistance partial factors for seismic assessment and retrofit. In 16th European conference on earthquake engineering, Thessaloniki
- Giongo I, Dizhur D, Tomasi R, Ingham JM (2013) In-plane assessment of existing timber diaphragms in URM buildings via quasi-static and dynamic in situ tests. *Adv Mater Res* 778:495–502. <https://doi.org/10.4028/www.scientific.net/AMR.778.495>
- GNDT (1994) Scheda Di Esposizione e Vulnerabilità e Di Rilevamento Danni Di Primo Livello e Secondo Livello (Muratura e Cemento Armato). Gruppo Nazionale per la Difesa dai Terremoti (GNDT), Roma (**In Italian**)
- Griffith MC, Lam NTK, Wilson JL, Doherty K (2004) Experimental investigation of unreinforced brick masonry walls in flexure. *J Struct Eng* 130(3):423–432. [https://doi.org/10.1061/\(ASCE\)0733-9445\(2004\)130:3\(423\)](https://doi.org/10.1061/(ASCE)0733-9445(2004)130:3(423))
- Grünthal G (1998) European macroseismic scale 1998: EMS-98. Chaiers du Centre Européen de Géodynamique et de Séismologie, Luxembourg
- INE (2012) Censos 2011 Resultados Definitivos—Portugal. Instituto Nacional de Estatística (INE), I.P. Lisboa (**in Portuguese**)
- IPQ (2010) Eurocódigo 8—Projecto de Estruturas Para Resistência Aos Sismos. Parte 1: Regras Gerais, Acções Sísmicas e Regras Para Edifícios, NP EN 1998-1:2010. Instituto Português da Qualidade (IPQ), Caparica (**in Portuguese**)
- IPQ (2017) Eurocódigo 8—Projeto de Estruturas Para Resistência Aos Sismos Parte 3: Avaliação e Reabilitação de Edifícios, NP EN 1998-3:2017. Instituto Português da Qualidade (IPQ), Caparica (**in Portuguese**)
- Joint Committee on Structural Safety (2011) Probabilistic model code. Part 3: Resistance models. 3.2. Masonry Properties. ISBN 978-3-909386-79-6
- Kržan M, Gostič S, Cattari S, Bosiljkov V (2015) Acquiring reference parameters of masonry for the structural performance analysis of historical buildings. *Bull Earthq Eng* 13(1):203–236. <https://doi.org/10.1007/s10518-014-9686-x>
- Lagomarsino S (2015) Seismic assessment of rocking masonry structures. *Bull Earthq Eng* 13(1):97–128. <https://doi.org/10.1007/s10518-014-9609-x>
- Lagomarsino S, Cattari S (2014) Fragility functions of masonry buildings. In: Ptilakis K, Crowley H, Kaynia A (eds) SYNER-G: typology definition and fragility functions for physical elements at seismic risk, buildings, lifelines, transportation networks and critical facilities, geotechnical, geological and earthquake engineering, vol 27. Springer, Berlin, pp 111–156. https://doi.org/10.1007/978-94-007-7872-6_5
- Lagomarsino S, Cattari S (2015) PERPETUATE guidelines for seismic performance-based assessment of cultural heritage masonry structures. *Bull Earthq Eng* 13(1):13–47. <https://doi.org/10.1007/s10518-014-9674-1>
- Lagomarsino S, Giovinazzi S (2006) Macroseismic and mechanical models for the vulnerability and damage assessment of current buildings. *Bull Earthq Eng* 4(September):415–443. <https://doi.org/10.1007/s10518-006-9024-z>
- Lagomarsino S, Penna A, Galasco A, Cattari S (2013) TREMURI program: an equivalent frame model for the nonlinear seismic analysis of masonry buildings. *Eng Struct* 56:1787–1799. <https://doi.org/10.1016/j.engstruct.2013.08.002>
- Liel AB, Haselton CB, Deierlein GG, Baker JW (2009) Incorporating modeling uncertainties in the assessment of seismic collapse risk of buildings. *Struct Saf* 31:197–211. <https://doi.org/10.1016/j.strusafe.2008.06.002>
- Lopes M, Meireles H, Cattari S, Bento R, Lagomarsino S (2014) Pombalino constructions: description and seismic assessment. In: Costa A, Guedes JM, Varum H (eds) Structural rehabilitation of old buildings, Building pathology and rehabilitation, vol 2, 1st edn. Springer, Berlin, pp 187–233. <https://doi.org/10.1007/978-3-642-39686-1>
- Lourenço PB, Mendes N, Ramos LF, Oliveira DV (2011) Analysis of masonry structures without box behavior. *Int J Archit Herit* 5:369–382. <https://doi.org/10.1080/15583058.2010.528824>
- Mendes N, Lourenço PB, Campos-Costa A (2014) Shaking table testing of an existing masonry building: assessment and improvement of the seismic performance. *Earthq Eng Struct Dyn* 43(2):247–266. <https://doi.org/10.1002/eqe.2342>

- MIT (2009) Istruzioni per l'applicazione Delle 'Norme Tecniche per Le Costruzioni' Di Cui Al Decreto Ministeriale 14/01/2008. Ministero delle Infrastrutture e dei Trasporti (MIT), Roma (**In Italian**)
- Morandi P, Albanesi L, Graziotti F, Li Piani T, Penna A, Magenes G (2018) Development of a dataset on the in-plane experimental response of URM piers with bricks and blocks. *Constr Build Mater* 190(2018):593–611
- NTC (2008) Norme Tecniche per Le Costruzioni (NTC). Decreto Ministeriale 14/01/2008. Roma (**In Italian**)
- NZSEE (2017) The seismic assessment of existing buildings. Technical guidelines for engineering assessments. Part C—Detailed seismic assessment. Part C8—Unreinforced masonry buildings. New Zealand Society for Earthquake Engineering (NZSEE) Inc., Wellington
- Rebello A, Guedes JM, Quelhas B, Ilharco T (2015) Assessment of the mechanical behaviour of Tabique walls through experimental tests. In Proceedings of the 2nd international conference on historic earthquake-resistant timber frames in the mediterranean region, Lisboa
- RGEUL (1930) Regulamento Geral Das Edificações Urbanas Em Lisboa (RGEUL). Postura da Câmara Municipal de Lisboa de 28/08/1930. Lisboa (**in Portuguese**)
- Rubinstein RY (2011) Simulation and the Monte Carlo method. Wiley, New York
- Simões A (2018) Evaluation of the seismic vulnerability of the unreinforced masonry buildings constructed in the transition between the 19th and 20th centuries in Lisbon, Portugal. Ph.D. Thesis. Instituto Superior Técnico, Universidade de Lisboa, Lisboa
- Simões A, Bento R, Cattari S, Lagomarsino S (2014a) Seismic assessment of 'Gaioleiro' buildings in Lisbon. In: Proceedings of the 9th international masonry conference, Guimarães
- Simões A, Bento R, Cattari S, Lagomarsino S (2014b) Seismic performance-based assessment of 'Gaioleiro' buildings. *Eng Struct* 80(December):486–500. <https://doi.org/10.1016/j.engstruct.2014.09.025>
- Simões A, Milošević J, Meireles H, Bento R, Cattari S, Lagomarsino S (2015) Fragility curves for old masonry building types in Lisbon. *Bull Earthq Eng* 13(10):3083–3105. <https://doi.org/10.1007/s10518-015-9750-1>
- Simões A, Appleton JG, Bento R, Caldas JV, Lourenço PB, Lagomarsino S (2017) Architectural and structural characteristics of masonry buildings between the 19th and 20th Centuries in Lisbon, Portugal. *Int J Archit Herit* 11(4):457–474. <https://doi.org/10.1080/15583058.2016.1246624>
- Simões A, Bento R, Lagomarsino S, Lourenço PB (2018) The seismic assessment of masonry buildings between the 19th and 20th centuries in Lisbon—evaluation of uncertainties. In Proceedings of the 10th international masonry conference, Milan
- Simões A, Bento R, Lagomarsino S, Cattari S, Lourenço PB (2019a) Fragility functions for tall URM buildings around early 20th century in Lisbon. Part 1: method description and application to a case study. *Int J Archit Herit* (Submitted)
- Simões A, Bento R, Lagomarsino S, Cattari S, Lourenço PB (2019b) Fragility functions for tall URM buildings around early 20th century in Lisbon. Part 2: application to different classes of buildings. *Int J Archit Herit* (Submitted)
- SVIBS (2013) ARTeMIS Modal Pro 3.0. Structural Vibration Solutions (SVIBS)
- Turnšek V, Čačovič F (1970) Some experimental results on the strength of brick masonry walls. In: Proceedings of the 2nd international brick masonry conference. Stoke-on-Trent
- Turnšek V, Sheppard P (1980) The shear and flexural resistance of masonry walls. In: Proceedings of the international research conference on earthquake engineering. Skopje
- Vanin F, Zaganelli D, Penna A, Beyer K (2017) Estimates for the stiffness, strength and drift capacity of stone masonry walls based on 123 quasi-static cyclic tests reported in the literature. *Bull Earthq Eng*. <https://doi.org/10.1007/s10518-017-0188-5>
- Vicente R, Parodi S, Lagomarsino S, Varum H, Mendes da Silva J (2011) Seismic vulnerability and risk assessment: case study of the Historic City Centre of Coimbra, Portugal. *Bull Earthq Eng* 9:1067–1096. <https://doi.org/10.1007/s10518-010-9233-3>
- Zhang P, Nagae T, McCormick J, Ikenaga M, Katsuo M, Nakashima M (2008) Friction-based sliding between steel and steel, steel and concrete, and wood and stone. In: Proceedings of the 14th world conference on earthquake engineering